

Observation of $B_s^0 \rightarrow D_s^- l^+ \nu X$ with $D_s^- \rightarrow \phi l^- \nu$

Paschal Coyle, CERN,
Christos Georgiopoulos and David E. Jaffe, SCRI, Florida State University,
Marie-Hélène Schune, LAL, Orsay

October 7, 1994

Abstract

The B_s^0 is observed in the decays of $B_s^0 \rightarrow D_s^- l^+ \nu X$ and $D_s^- \rightarrow \phi l^- \nu$ in approximately 1.64 million hadronic Z decays. The number of B_s^0 found after subtraction of backgrounds is 17.7 ± 6.7 (stat) ± 1.1 (syst). Monte Carlo studies show that the decay length and boost resolution are nearly identical to that obtained for $B_s^0 \rightarrow D_s^- l^+ \nu X$ when the D_s^+ is fully reconstructed.

1 Introduction

Reconstruction of the decay modes of the D_s^+ is of interest in the study of B_s^0 $-\bar{B}_s^0$ mixing and measurements of the B_s^0 lifetime [1]. CLEO recently reported a measurement of the branching ratio of $D_s^- \rightarrow \phi e^- \nu$ with respect to the popular $\phi\pi^+$ mode of $0.54 \pm 0.05 \pm 0.04$ [2] which indicates that ϕ, l^+, l^- correlations should yield roughly the same number of semileptonic B_s^0 decays as the $\phi\pi^+$.

2 Selection criteria

Approximately 1.64 million hadronic Z decays with the VDET operational were selected from the 1991, 1992 and 1993 MINIs.

Good tracks with momenta greater than (2)3 GeV and satisfying the standard heavy flavor criteria were selected as (electron)muon candidates.[3] Additional electron candidates were identified as tracks satisfying the standard electron criteria with momenta between 1.0 and 2.0 GeV where the dE/dx was present (> 50 samples) and inconsistent with the proton hypothesis at more than 2σ ($|\chi_p| > 2.0$).

Good, non-lepton tracks with momenta greater than 1.5 GeV were selected as kaon candidates and $\chi_K + \chi_\pi < 1$ was required if the dE/dx information was present.

To constrain the four tracks to be in the same jet, the cosine of the angle between each pair of tracks was required to be greater than 0.7. The following criteria were also applied (with the notation that $l_{1(2)}$ is the D_s^+ (B_s^0) daughter):

1. No additional leptons in the same hemisphere as the ϕ, l^+, l^- candidate,
2. $M(\mu^+, \mu^-)$ inconsistent with the J/ψ and ψ' masses at ± 100 MeV,

3. $M(e^+, e^-)$ inconsistent with the J/ψ and ψ' masses at ± 100 MeV and greater than 100 MeV to exclude photon conversions,
4. $P(\phi) > 4.0$ GeV,
5. $M(\phi, l_1) < M(D_s^+) - \Delta$ and $M(\phi, l_2) > M(D_s^+) + \Delta$ with $\Delta = 15$ MeV, to unambiguously assign l_1 and l_2 (see Figure 1). This cut is essential for a B_s^0 oscillation measurement,
6. $P(l_2) > 3.0$ GeV,
7. l_2 and at least 2 of the 3 "D_s" daughters must have at least one VDET hit in both the $r\phi$ and z views, where "D_s" $\equiv \phi, l_1$,
8. Probability of χ^2 for the ϕ, l_1 and "D_s", l_2 vertices was required to be greater than 0.01%,
9. $2.5 < M(\phi, l_1, l_2) < 5.5$ GeV and
10. $P(l_2) > 5$ GeV or $E_{\text{miss}} > 10$ GeV, where E_{miss} is the missing energy in the same hemisphere.

The last cut (10) reduces the $B \rightarrow D_s^{(*)-} \bar{D}^{(*)} X$ background as well as the combinatorial background by taking advantage of the larger missing energy in the $B_s^0 \rightarrow D_s^- l^+ \nu$ ($D_s^- \rightarrow \phi l^- \nu$) events as can be seen graphically in Figure 2. The detection efficiencies as determined from dedicated Monte Carlo of signal and background processes are shown in Table 1. In each dedicated Monte Carlo, $\mathcal{B}(D_s^+ \rightarrow \phi e^+ \nu) = \mathcal{B}(D_s^+ \rightarrow \phi \mu^+ \nu) = 50\%$ and $\mathcal{B}(\phi \rightarrow K^+ K^-) = 100\%$. In the $B^0 \rightarrow D_s^- D^+$ and $B^0 \rightarrow D_s^{*-} D^{*+}$ Monte Carlos, the D^+ was forced to decay semileptonically according to the standard HVFL04 branching ratios and $\mathcal{B}(D^{*+} \rightarrow D^+ \pi^0) = 100\%$ in the $B^0 \rightarrow D_s^{*-} D^{*+}$ Monte Carlo. Finally, in the $B \rightarrow D_s^- K l^+ \nu$ Monte Carlo, $\mathcal{B}(B^{0(+)} \rightarrow D_s^+ K^{0(+)} e^- \nu) = \mathcal{B}(B^{0(+)} \rightarrow D_s^+ K^{0(+)} \mu^- \nu) = 50\%$. The resulting ϕ, l^+, l^- mass distributions are shown in Figure 3.

3 Results

As shown in Figure 4A, the pull on the decay length resolution is centered at zero (0.04 ± 0.05) and represented by a gaussian of sigma 1.24 ± 0.04 which are both consistent with the results for the fully-reconstructed D_s^+ modes [1]. The decay length resolution, Figure 4B, is also consistent with [1]. In the κ distribution¹ in Figure 4C, $83.5 \pm 1.3\%$ of the events are contained within a gaussian core of 5% which is consistent with the results in [1] while the mean(RMS) is approximately 2% (7.5%) larger than for the fully-reconstructed D_s^+ modes.

The $K^+ K^-$ mass distributions with the above cuts for the like- and unlike-sign lepton combinations are shown in Figure 5A. A simple Breit-Wigner was found to give a reasonable fit to the simulated data and is used to represent the ϕ peak in the fits shown. (Fitting the width and mass gave $\Gamma = 5.6_{-1.7}^{+2.3}$ MeV and $\langle M \rangle = 1019.4_{-0.9}^{+1.1}$ MeV consistent with $\Gamma = 4.7$ MeV from Monte Carlo and $M(\phi) = 1019.413 \pm 0.008$ MeV [4].) A second-order polynomial is used to fit the background. There are 37(8) ϕ, l^+, l^- (ϕ, l^\pm, l^\pm) events within 6 MeV of the ϕ mass. Subtracting the fitted number of background events from the data events in this mass range gives $25.8 \pm 6.9 \pm 0.5$

¹The B_s^0 momentum is reconstructed using the procedure described in [1]

ϕ, l^+, l^- and $5.4 \pm 3.3 \pm 0.1 \phi, l^\pm, l^\pm$ candidates where the systematic uncertainty is estimated by a linear background fit. Using the ϕ, l^\pm, l^\pm events as an estimate of the “fake” lepton background gives $20.4 \pm 7.7 \pm 0.5$ candidates. With the conservative assumptions that 100% of $\mathcal{B}(B \rightarrow D_s^+ X) = 11.81 \pm 0.43 \pm 0.94\%$ [5] proceeds through $B \rightarrow D_s^{(*)-} \bar{D}^{(*)} X$, the number of ϕ, l^+, l^- candidates from $B_s^0 \rightarrow D_s^- l^+ \nu X$ is $17.7 \pm 6.7(\text{stat}) \pm 1.1(\text{syst})$ where the systematic uncertainty includes the uncertainty in the relative $B \rightarrow D_s^{(*)-} \bar{D}^{(*)} X$ and $B_s^0 \rightarrow D_s^- l^+ \nu X$ rates and the uncertainty in the background fit. This estimate neglects possible background from the as yet unobserved[6] $B \rightarrow D_s^- K l^+ \nu$ channel which is expected to be very small[7].

A greater yield of ϕ, l^+, l^- is observed with a severe degradation of the decay length resolution and an increase in the relative $B \rightarrow D_s^{(*)-} \bar{D}^{(*)} X$ efficiency when cuts (7) and (8) are omitted as shown in Figure 5B. There are $52.4 \pm 11.3 \pm 1.6 \phi, l^+, l^-$ and $5.9 \pm 5.1 \pm 0.5 \phi, l^\pm, l^\pm$ background-subtracted events within 6 MeV of the ϕ mass. In this case the yield of ϕ, l^+, l^- from $B_s^0 \rightarrow D_s^- l^+ \nu X$ is found to be $39.5 \pm 10.5 \pm 2.9$ after the like-sign and $B \rightarrow D_s^{(*)-} \bar{D}^{(*)} X$ subtraction.

References

- [1] Measurement of the B_s^0 lifetime, ALEPH Collaboration, D. Buskulic *et.al.*, Phys. Lett. **B322** (1994) 275, and the corresponding ALEPH note, Colas *et.al.*, ALEPH 93-116, 14 July 1993.
- [2] A measurement of $\mathcal{B}(D_s^+ \rightarrow \phi l^+ \nu) / \mathcal{B}(D_s^+ \rightarrow \phi \pi^+)$, CLEO Collaboration, F. Butler *et.al.*, Preprint CLNS94-1272, 25 Jan 1994.
- [3] Heavy quark tagging with leptons in the ALEPH detector, D. Buskulic *et.al.*, Nucl. Inst. and Meth. **A346** (1994) 461.
Electrons: $-1.8 < R_L < 3.0$, $-1.6 < R_T$ and $-2.5 < R_1$ (if dE/dx available).
Muons: QMUIDO identification flag > 12 .
- [4] Review of Particle Properties, Particle Data Group, Phys. Rev. **D45** June 1992.
- [5] Measurement of $B \rightarrow D_s^+ X$ Decays, CLEO Collaboration, T. Bergfeld *et.al.*, Submitted to ICHEP94, Glasgow, CLEO CONF 94-9. Assumes $\mathcal{B}(D_s^+ \rightarrow \phi \pi^+) = 3.7 \pm 0.9\%$.
- [6] Search for Rare B Meson decays into D_s^+ Mesons, ARGUS Collaboration, H. Albrecht *et.al.*, Preprint DESY 93-054, April 1993.
- [7] Backgrounds for tagging B_s^0 at LEP, E. Golowich *et.al.*, Z. Phys. **C48** (1990) 89.

Relative detection efficiency in %				
D_s^+ decay mode	$B_s^0 \rightarrow D_s^- l^+ \nu$	$B^0 \rightarrow D_s^- D^+$	$B^0 \rightarrow D_s^{*-} D^{*+}$	$B \rightarrow D_s^- K l^+ \nu$
$\phi e^- \nu$	6.69 ± 0.31	1.62 ± 0.23	0.96 ± 0.18	3.02 ± 0.25
$\phi \mu^- \nu$	4.51 ± 0.24	1.01 ± 0.17	0.67 ± 0.15	1.50 ± 0.18
Relative efficiency of cut 10 in %				
$\phi e^- \nu$	94.6 ± 1.1	72.5 ± 5.4	82.9 ± 6.4	90.6 ± 2.3
$\phi \mu^- \nu$	93.9 ± 1.3	71.4 ± 6.5	76.9 ± 8.3	92.3 ± 3.0

Table 1: The relative detection efficiency for the signal, $B_s^0 \rightarrow D_s^- l^+ \nu$, and various background channels. The relative efficiency of cut (10) ($P(l_2) > 5$ GeV or $E_{\text{miss}} > 10$ GeV) is also shown.

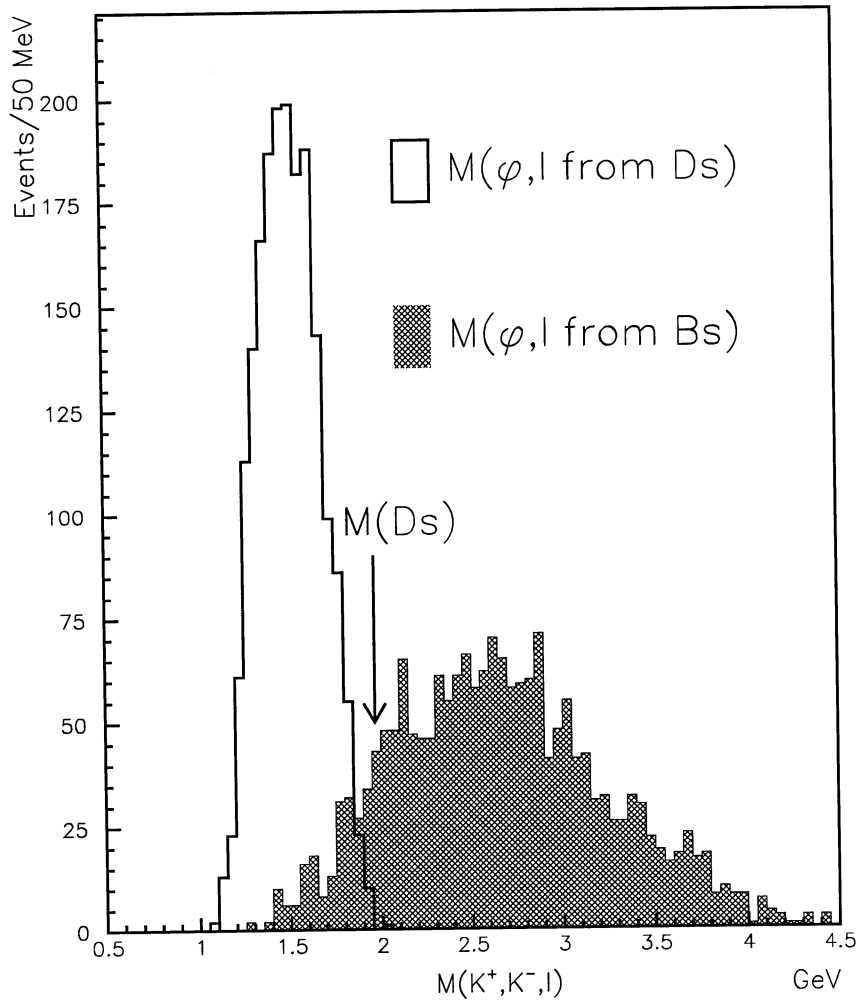


Figure 1: The ϕ , lepton mass distributions for reconstructed and matched $B_s^0 \rightarrow D_s^- l^+ \nu$ ($D_s^- \rightarrow \phi l^- \nu$) decays after cuts (4) and (6) showing the effectiveness of cut (5) to assign l_1 and l_2 . The relative efficiency of cut (5) is $87.6 \pm 0.7\%$.

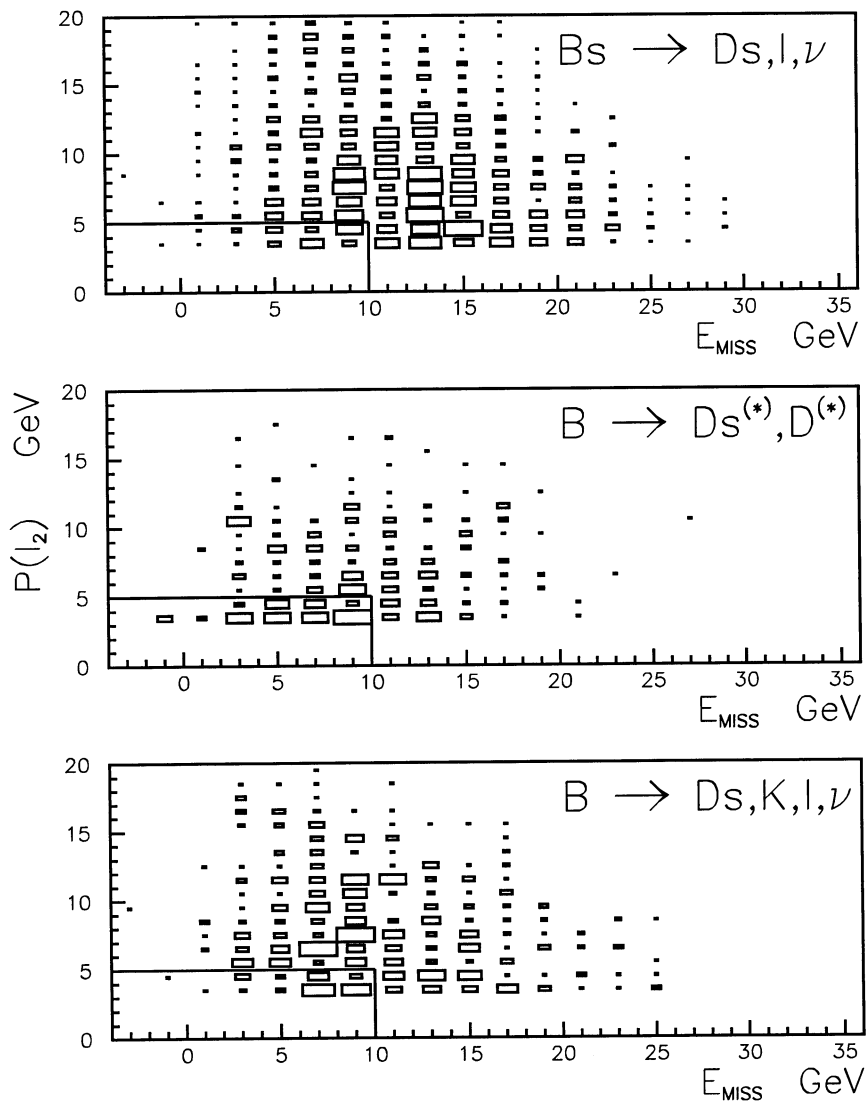


Figure 2: The $P(l_2)$ vs. E_{miss} distributions for the processes $B_s^0 \rightarrow D_s^- l^+ \nu$, $B \rightarrow D_s^{(*)-} \bar{D}^{(*)} X$ and $B \rightarrow D_s^- K l^+ \nu$ where the $B \rightarrow D_s^{(*)-} \bar{D}^{(*)} X$ distribution includes the contributions from $B^0 \rightarrow D_s^- D^+$ and $B^0 \rightarrow D_s^{*-} D^{*+}$. The box in the lower left corner shows the events excluded by cut (10).

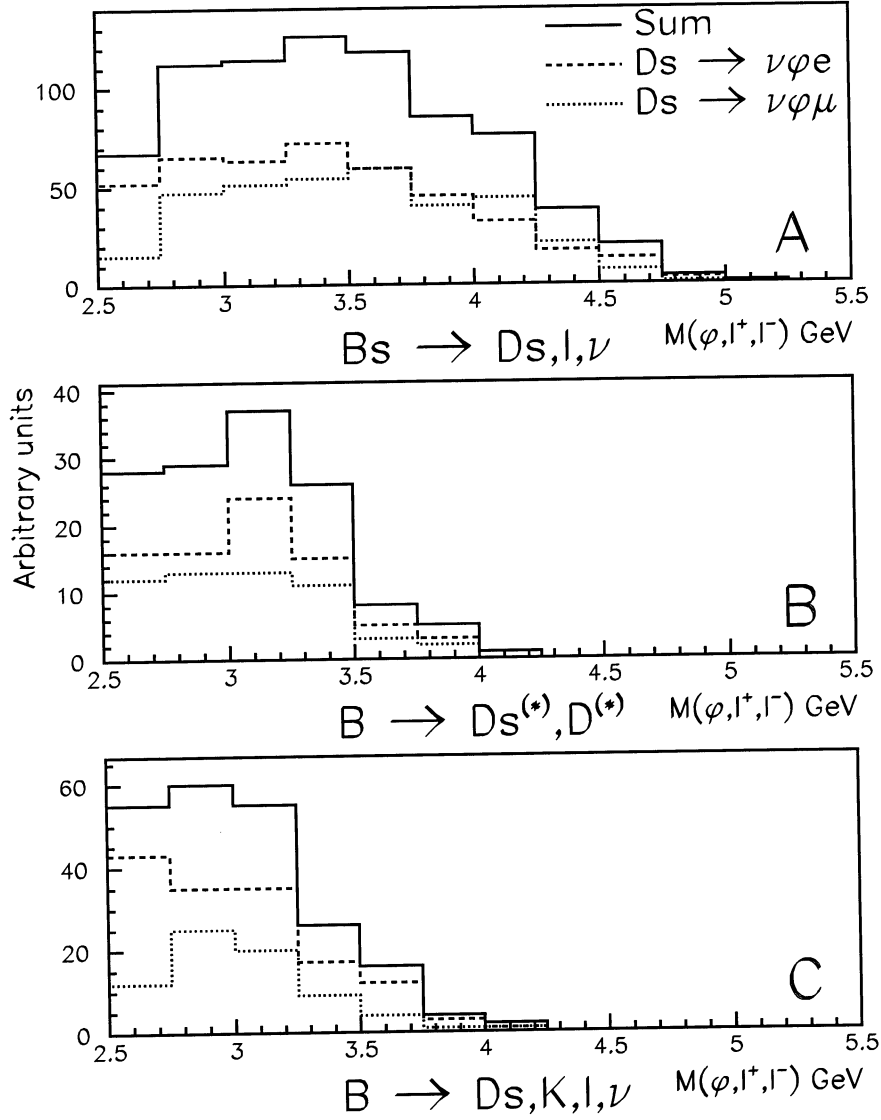


Figure 3: The ϕ, l^+, l^- mass spectra for the processes A) $B_s^0 \rightarrow D_s^- l^+ \nu$, B) $B \rightarrow D_s^{(*)} \bar{D}^{(*)} X$ and C) $B \rightarrow D_s^- K l^+ \nu$ showing the individual contributions from $D_s^- \rightarrow \phi e^- \nu$ and $D_s^- \rightarrow \phi \mu^- \nu$. The $B \rightarrow D_s^{(*)} \bar{D}^{(*)} X$ distribution includes the contributions from $B^0 \rightarrow D_s^- D^+$ and $B^0 \rightarrow D_s^{*-} D^{*+}$.

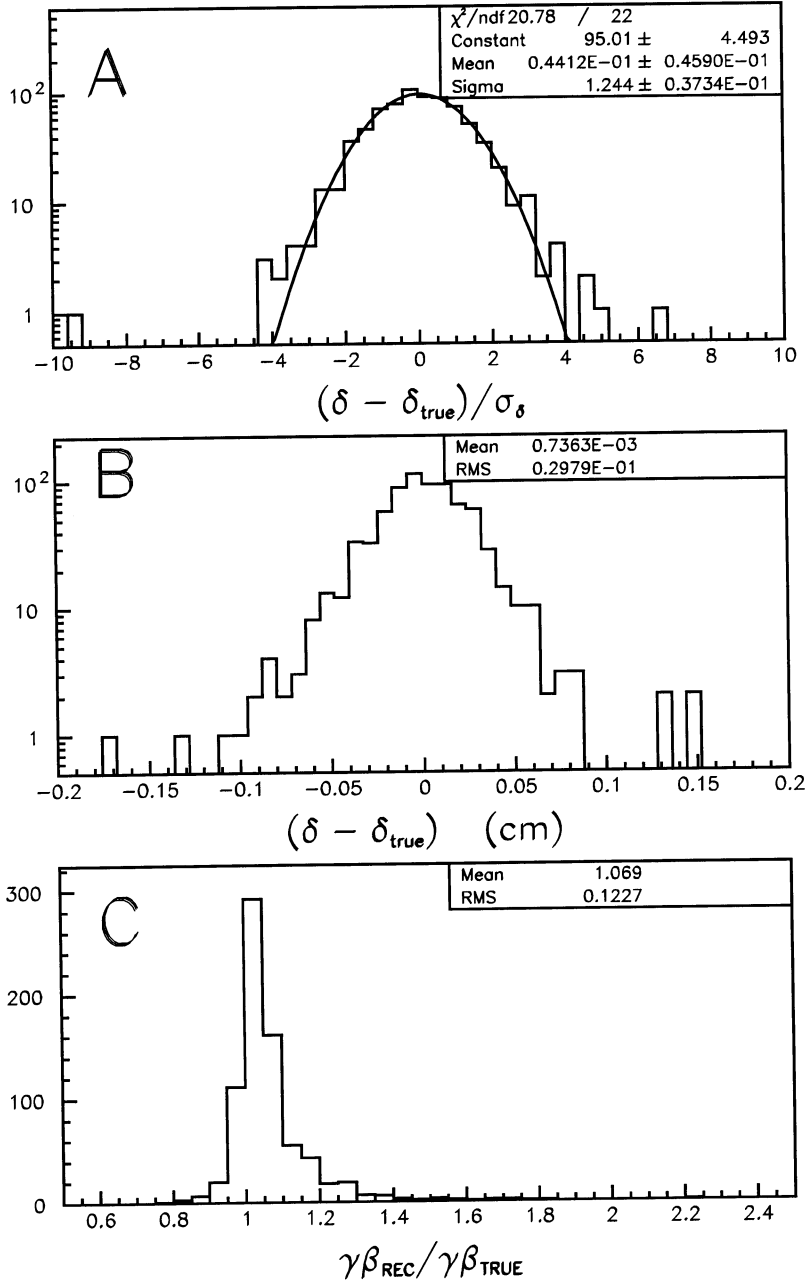


Figure 4: The A) pull on the ϕ, l^+, l^- decay length resolution, B) ϕ, l^+, l^- decay length resolution and C) boost resolution.

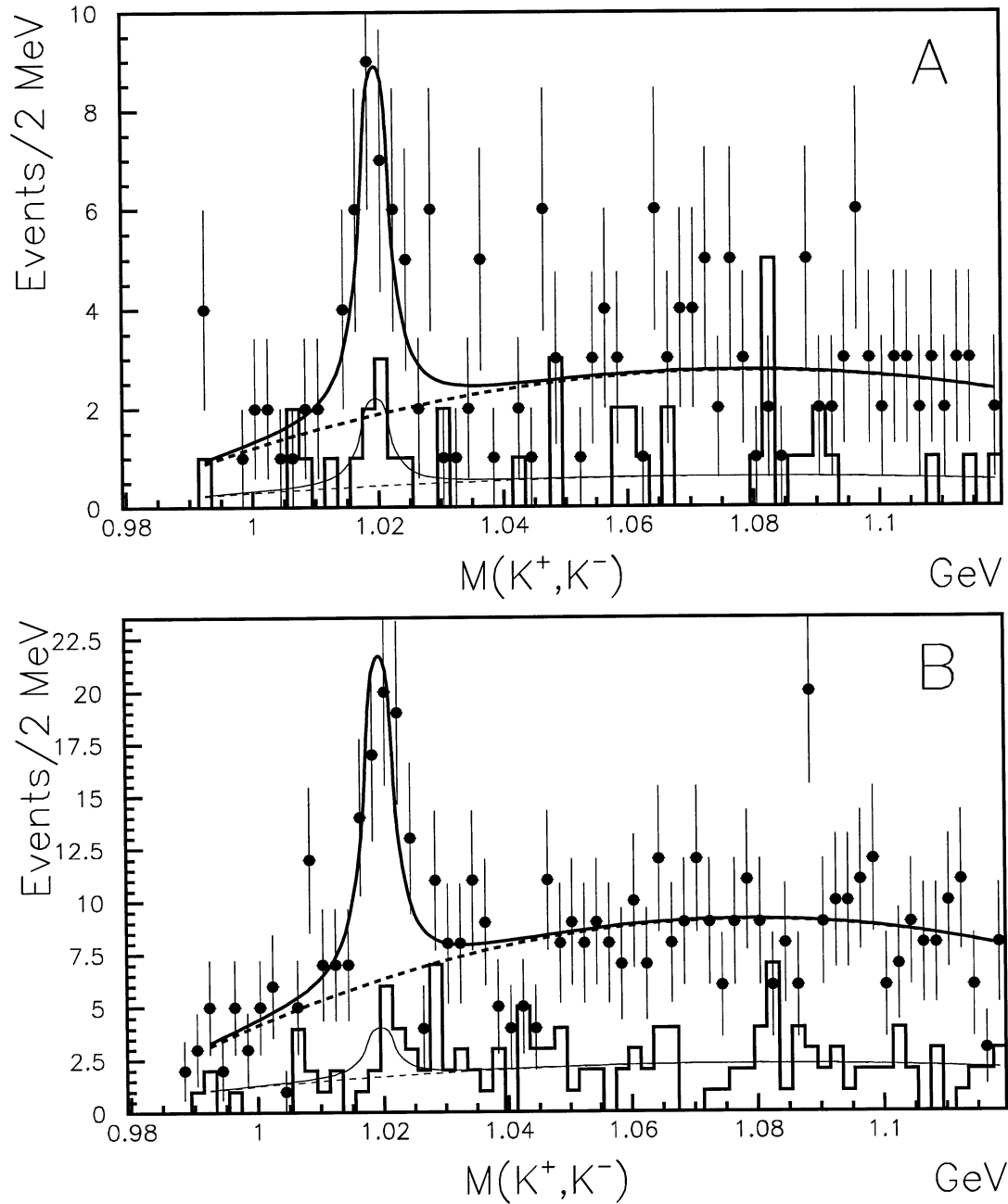


Figure 5: A) The points(histogram) represent $M(K^+K^-)$ distribution for $l^+l^- (l^\pm l^\pm)$ combinations. The solid line shows the result of a binned, maximum likelihood fit to a second order polynomial to represent the background and a Breit-Wigner for the signal with the known ϕ mass and Γ fixed at the value expected from the simulation. The dashed lines shows the fitted background. B) The mass spectra without the cuts on the VDET and probability of χ^2 for the vertices.